Article

The Structure of a Mixed LNA/DNA:RNA Duplex Is Driven by Conformational Coupling between LNA and Deoxyribose Residues as Determined from ^{13}C Relaxation Measurements

Katrine E. Nielsen, and H. Peter Spielmann

J. Am. Chem. Soc., **2005**, 127 (43), 15273-15282• DOI: 10.1021/ja051026z • Publication Date (Web): 07 October 2005

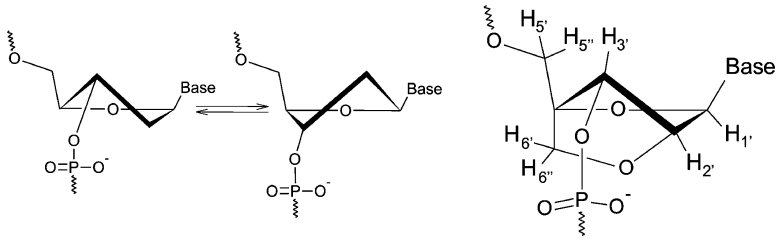

More About This Article

Additional resources and features associated with this article are available within the HTML version:

- Supporting Information
- Links to the 1 articles that cite this article, as of the time of this article download
- Access to high resolution figures
- Links to articles and content related to this article
- Copyright permission to reproduce figures and/or text from this article

View the Full Text HTML

J|A|C|S
ARTICLES
Published on Web 10/07/2005

The Structure of a Mixed LNA/DNA:RNA Duplex Is Driven by Conformational Coupling between LNA and Deoxyribose Residues as Determined from ^{13}C Relaxation Measurements

Katrine E. Nielsen[†] and H. Peter Spielmann*[,‡]

Contribution from the Department of Molecular and Cellular Biochemistry, Department of Chemistry, and Kentucky Center for Structural Biology, University of Kentucky, Lexington, Kentucky 40536-0084, and Nucleic Acid Center, Department of Chemistry, University of Southern Denmark, Campusvej 55, DK-5230 Odense M, Denmark

Received February 17, 2005; E-mail: hps@uky.edu

Abstract: A study of the internal dynamics of an LNA/DNA:RNA duplex has been performed to further characterize the conformational changes associated with the incorporation of locked nucleic acid (LNA) nucleotides in a DNA:RNA duplex. In general, it was demonstrated that the LNA/DNA:RNA duplex has a very high degree of order compared to dsDNA and dsRNA duplexes. The order parameters of the aromatic carbon atoms in the LNA/DNA strand are uniformly high, whereas a sharp drop in the degree of order was seen in the RNA strand in the beginning of the AUAU stretch in the middle of the strand. This can be related to a return to normal dsRNA dynamics for the central A:U base pair. The high order of the heteroduplex is consistent with preorganization of the chimera strand for an A-form duplex conformation. These results partly explain the dramatic increase in T_m of the chimeric heteroduplex over dsDNA and DNA:RNA hybrids of the same sequence.

Introduction

The translation of proteins can be efficiently blocked by the antisense targeting of messenger RNA with small single-stranded nucleic acids.[1−3] Antisense molecules operate by directly blocking the translational apparatus or promoting cleavage of the target RNA by RNase H.[4,5] Small single-stranded antisense DNAs and RNAs can bind selectively to mRNA and, in the case of antisense DNA, promote RNase H activity. However, delivery of antisense DNA and RNA is difficult as they are susceptible to degradation by intra- and extracellular nucleases and cross the cellular membrane inefficiently. These difficulties have prompted the development of a wide range of chemically modified nucleic acid analogues with enhanced stability and nucleic acid binding properties.[6−8] For example, the phosphorothioate modified DNA 21-mer antisense drug, Vitravene, is now available to treat cytomegalovirus retinitis in AIDS patients.[9] Chemically modified oligonucleotides with enhanced binding properties and increased selectivity toward target nucleic acid sequences are also useful research tools for molecular biology.[10−12]

Recently, the conformationally rigid bicyclic locked nucleic acid (LNA) nucleotide analogue (Chart 1) was developed.[13−16] The LNA nucleotide adopts an RNA-like *N*-type sugar conformation, as opposed to the *S*-type sugar conformation preferred by deoxyribonucleotides in dsDNA. Chimeric oligonucleotides composed of LNA and mixed LNA/DNA sequences are attractive for antisense applications because they are more stable to 3′-exonucleolytic degradation, are able to cross the cell membrane, and exhibit low in vivo toxicity.[17] The ability of chimeric LNA/DNA sequences to elicit RNase H-mediated cleavage of the RNA strand depends on the specific sequence and composition of the antisense oligonucleotide.[17,18] Relative to DNA oligonucleotides, LNA oligonucleotides have increased binding affinity toward complementary RNA or DNA.[19,20]

[†] University of Southern Denmark.
[‡] University of Kentucky.

(1) Paterson, B. M.; Roberts, B. E.; Kuff, E. L. *Proc. Natl. Acad. Sci. U.S.A.* **1977**, *74*, 4370−4374.
(2) Stephenson, M. L.; Zamecnik, P. C. *Proc. Natl. Acad. Sci. U.S.A.* **1987**, *75*, 285−288.
(3) Simons, R. W.; Kleckner, N. *Cell* **1983**, *34*, 683−691.
(4) Crooke, S. T. *Biochim. Biophys. Acta* **1999**, *1489*, 31−44.
(5) Baker, B. F.; Monia, B. P. *Biochim. Biophys. Acta* **1999**, *1489*, 3−18.
(6) Freier, S. M.; Altmann, K.-H. *Nucleic Acids Res.* **1997**, *25*, 4429−4443.
(7) Wilds, C. J.; Minasov, G.; Natt, F.; von Matt, P.; Altmann, K.-H.; Egli, M. *Nucleosides, Nucleotides Nucleic Acids* **2001**, *20*, 991−994.
(8) Micklefield, J. *Curr. Med. Chem.* **2001**, *8*, 1157−1179.
(9) Henry, S. P.; Miner, R. C.; Drew, W. L.; Fitchett, J.; York-Defalco, C.; Rapp, L. M.; Levin, A. A. *Invest. Ophthalmol. Visual Sci.* **2001**, *42*, 2646−2651.
(10) Simeonov, A.; Nikiforov, T. T. *Nucleic Acids Res.* **2002**, *30*, e91.
(11) Nielsen, P. E. *Curr Opin. Biotechnol.* **2001**, *12*, 16−20.
(12) Kroger, K.; Jung, A.; Reder, S.; Gauglitz, G. *Anal. Chim. Acta* **2002**, *469*, 37−48.
(13) Singh, S. K.; Nielsen, P.; Koshkin, A. A.; Wengel, J. *Chem. Commun.* **1998**, 455−456.
(14) Koshkin, A. A.; Singh, S. K.; Nielsen, P.; Rajwanshi, V. K.; Kumar, R.; Meldgaard, M.; Olsen, C. E.; Wengel, J. *Tetrahedron* **1998**, *54*, 3607−3630.
(15) Koshkin, A. A.; Rajwanshi, V. K.; Wengel, J. *Tetrahedron Lett.* **1998**, *39*, 4381−4384.
(16) Obika, S.; Nanbu, D.; Hari, Y.; Andoh, J.; Morio, K.; Doi, T.; Imanishi, T. *Tetrahedron Lett.* **1998**, *39*, 5401−5404.
(17) Wengel, J. et al. *Proc. Natl. Acad. Sci. U.S.A.* **2000**, *97*, 5633−5638.
(18) Kurreck, J.; Wyszko, E.; Gillen, C.; Erdmann, V. A. *Nucleic Acids Res.* **2002**, *30*, 1911−1918.
(19) Singh, S. K.; Wengel, J. *Chem. Commun.* **1998**, 1247−1248.
(20) Koshkin, A. A.; Nielsen, P.; Meldgaard, M.; Rajwanshi, V. K.; Singh, S. K.; Wengel, J. *J. Am. Chem. Soc.* **1998**, *120*, 13252−13253.

Chart 1. Chemical Structure and Numbering Scheme of LNA[a]

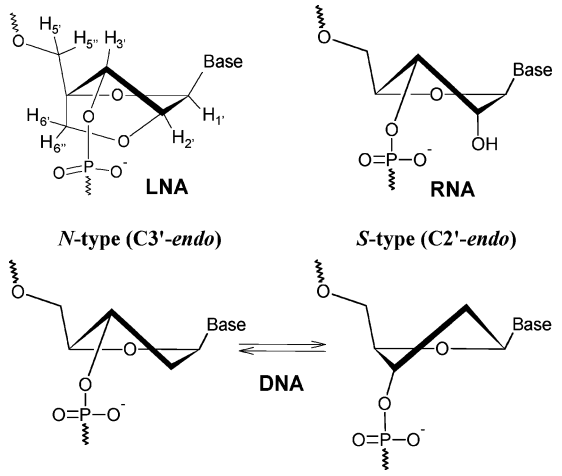

[a] LNA and RNA are fixed in an *N*-type conformation, whereas DNA usually exists in a dynamic equilibrium between *N*- and *S*-type sugar conformations.

The structural impact of LNA nucleotides incorporated into LNA/DNA chimeras hybridized with unmodified RNA or DNA has been studied by NMR.[21−26] Duplex molecules of LNA/DNA chimeras hybridized with unmodified RNA or DNA adopt an A-form-like structure. This is in contrast to the B-form structure adopted by DNA:DNA duplexes and the hybrid A−B-form structure of DNA:RNA duplexes.[27,28]

Nucleic acids are conformationally heterogeneous, and their interaction with other macromolecules is dependent on the conformations that they can adopt. The time averaged structure of double-stranded nucleic acids can be described with high accuracy by both NMR and X-ray crystallographic methods. However, nucleic acids exist in solution as a family (envelope) of closely related rapidly interconverting conformations characterized by changes in various sugar−phosphate backbone torsions. In particular, the sugar ring can interconvert via pseudorotation, the phosphodiester linkage interconvert between BI and BII and various other low amplitude vibrational modes in the bases, sugars, and backbone phosphates. Some of these motions appear to be conformationally coupled to each other.[29,30]

The conformational preference of the deoxyribose in DNA is dependent on the sequence context and identity of the base. In general, purines show a high population of *S*-type sugar ring conformation while pyrimidines have *N*-type conformational populations higher than those of purine nucleotides, although the *S*-type conformation predominates.[31] The deoxyribose conformational preferences are reflected in the global B-type conformation of DNA duplexes. On the other hand, the ribose residues in RNA show a strong preference for the *N*-type conformation due to the 2′-hydroxyl group.[31−33] As a result, duplex RNA has an A-type conformation. Interestingly, DNA:RNA heteroduplexes have conformations intermediate between the A- and B-forms. In solution, the RNA strand is found in the A-form conformation, whereas the deoxyribose residues of the DNA strand appear to interconvert between the C3′-endo/C2′-endo (*N*/*S*) conformations. The net result is an average helical conformation intermediate between the A- and B-forms.[27,28,34−37]

Inclusion of one or more LNA sugars into a DNA strand shifts the conformational preference of adjacent deoxyribonucleotides toward the *N*-type sugar ring conformations from the preferred *S*-type sugar ring conformation observed in dsDNA and RNA:DNA hybrids.[22−24]

Of particular interest is how the chemical modification of nucleic acids affects the conformational flexibility of the polymer, how these alterations are transmitted to adjacent nucleotides, and how they affect the average structure and envelope of available interconverting conformations. The interconversion of the sugar conformations occurs on the nanosecond to picosecond time scale, which makes an NMR investigation of these dynamic processes particularly informative.

Previous studies of nucleic acid dynamics employing ^{13}C relaxation have been performed with both natural abundance and ^{13}C enriched samples.[38−50] Relaxation studies with ^{13}C at natural abundance require very long data acquisition periods to achieve a satisfactory signal-to-noise ratio. However, this disadvantage is more than offset by allowing the simultaneous sampling of all spectroscopically resolved methine carbons in the molecule as well as avoiding the complications of $^{13}C-^{13}C$ cross-relaxation and the introduction of $^{13}C-^{13}C$ couplings into the nucleotide spin system. Furthermore, unnatural nucleotides are only available with either site-specific or uniform ^{13}C enrichment through prohibitively expensive organic synthesis.

(21) Nielsen, C. B.; Singh, S. K.; Wengel, J.; Jacobsen, J. P. *J. Biomol. Struct. Dyn.* **1999**, *17*, 175−191.
(22) Nielsen, K. E.; Singh, S. K.; Wengel, J.; Jacobsen, J. P. *Bioconjugate Chem.* **2000**, *11*, 228−238.
(23) Petersen, M.; Nielsen, C. B.; Nielsen, K. E.; Jensen, G. A.; Bondensgaard, K.; Singh, S. K.; Rajwanshi, V. K.; Koshkin, A. A.; Dahl, B. M.; Wengel, J.; Jacobsen, J. P. *J. Mol. Recognit.* **2000**, *13*, 44−53.
(24) Bondensgaard, K.; Petersen, M.; Singh, S. K.; Rajwanshi, V. K.; Kumar, R.; Wengel, J.; Jacobsen, J. P. *Chem.−Eur. J.* **2000**, *6*, 2687−2695.
(25) Jensen, G. A.; Singh, S. K.; Kumar, R.; Wengel, J.; Jacobsen, J. P. *J. Chem. Soc., Perkin Trans. 2* **2001**, 1224−1232.
(26) Petersen, M.; Bondensgaard, K.; Wengel, J.; Jacobsen, J. P. *J. Am. Chem. Soc.* **2002**, *124*, 5974−5982.
(27) Fedoroff, O. Y.; Salazar M.; Reid, B. R. *J. Mol. Biol.* **1993**, *233*, 509−523.
(28) Gonzalez, C.; Stec, W.; Reynolds, M. A.; James T. L. *Biochemistry* **1995**, *34*, 4969−4982.
(29) El Hassan, M. A.; Calladine, C. R. *Philos. Trans. R. Soc. London, Ser. A* **1997**, *355*, 43−100.
(30) Packer, J. M.; Hunter, C. A. *J. Mol. Biol.* **1998**, *280*, 407−420.
(31) Foloppe, N.; MacKerell, A. D., Jr. *Biophys. J.* **1999**, *76*, 3206−3218.
(32) Brameld, K. A.; Goddard, W. A., III. *J. Am. Chem. Soc.* **1999**, *121*, 985−993.
(33) Foloppe, N.; Nilsson, L.; Mackerell, A. D., Jr. *Biopolymers* **2001**, *61*, 61−76.
(34) Gyi, J. I.; Conn, G. L.; Lane, A. N.; Brown, T. *Biochemistry* **1996**, *35*, 4969−4982.
(35) Gyi, J. I.; Lane, A. N.; Conn, G. L.; Brown, T. *Biochemistry* **1998**, *37*, 73−80.
(36) Lane, A. N.; Ebel, S.; Brown, T. *Eur. J. Biochem.* **1993**, *215*, 297−306.
(37) Horton, N. C.; Finzel, B. C. *J. Mol. Biol.* **1996**, *264*, 521−533.
(38) Michnicka, M. J.; Harper, J. W.; King, G. C. *Biochemistry* **1993**, *32*, 395−400.
(39) Dayie, K. T.; Brodsky, A. S.; Williamson, J. R. *J. Mol. Biol.* **2002**, *317*, 263−278.
(40) Legault, P.; Hoogstraten, C. G.; Metlitzky, E.; Pardi, A. *J. Mol. Biol.* **1998**, *284*, 325−335.
(41) Spielmann, H. P. *Biochemistry* **1998**, *37*, 5426−5438.
(42) Isaacs, R. J.; Rayens, W. S.; Spielmann, H. P. *J. Mol. Biol.* **2002**, *319*, 191−207.
(43) Spielmann, H. P. *Biochemistry* **1998**, *37*, 16863−16876.
(44) King, G. C.; Harper, J. W.; Xi, Z. *Methods Enzymol.* **1995**, *261*, 436−450.
(45) Akke, M.; Fiala, R.; Jiang, F.; Patel, D.; Palmer, A. G., III. *RNA* **1997**, *3*, 702−709.
(46) Hall, K. B.; Tang, C. *Biochemistry* **1998**, *37*, 9323−9332.
(47) Borer, P. N.; LaPlante, S. R.; Kumar, A.; Zanatta, N.; Martin, A.; Hakkinen, A.; Levy, G. C. *Biochemistry* **1994**, *33*, 2441−2450.
(48) Kojima, C.; Ono, A.; Kainosho, M.; James, T. L. *J. Magn. Reson.* **1999**, *136*, 169−175.
(49) Kojima, C.; Ulyanov, N. B.; Kainosho, M.; James, T. L. *Biochemistry* **2001**, *40*, 7239−7246.
(50) Kojima, C.; Ono, A.; Kainosho, M.; James, T. L. *J. Magn. Reson.* **1998**, *135*, 310−333.

Chart 2. Numbering Scheme and Sequence of the LNA/DNA:RNA Duplex[a]

	1	2	3	4	5	6	7	8	9	
5'-d(	C	$\mathbf{T^L}$	G	A	$\mathbf{T^L}$	A	$\mathbf{T^L}$	G	C	)-3'
3'-r(	G	A	C	U	A	U	A	C	G	)-5'
	18	17	16	15	14	13	12	11	10	

[a] $\mathbf{T^L}$ denotes an LNA thymine residue.

To gain a more complete understanding of the effect of the unnatural LNA sugar on nucleic acid structure, we report the internal dynamics of a chimeric LNA/DNA:RNA duplex containing three LNA nucleotides (Chart 2). The average solution structure of this LNA/DNA:RNA duplex has previously been determined.[26] We have measured natural abundance ^{13}C relaxation for spectroscopically resolved methines from which we have calculated order parameters that reflect the internal picosecond−nanosecond dynamics of the LNA/DNA:RNA duplex. We interpret these data to describe the effect of internal dynamics on the observed solution structure and behavior.

Experimental Section

Sample Preparation. The modified oligonucleotide was synthesized as previously described[13,14] and purified by ultracentrifugation using Microsep 1 K omega centrifugal devices (Pall Life Sciences). The duplex molecule was prepared by dissolving equimolar amounts of the two single strands in 0.6 mL of 10 mM sodium phosphate buffer (pH 7.0), 100 mM NaCl, and 0.05 mM NaEDTA. The sample was lyophilized three times from D_2O and redissolved in 99.96% D_2O (Cambridge Isotope Laboratories). The final concentration of the duplex was 4 mM.

NMR Experiments. All NMR experiments were performed on a Varian Unity 500 spectrometer at 25 °C. The ^{13}C spin−lattice (R_1), spin−spin (R_2) relaxation rate constants, and steady-state $\{^1H\}-^{13}C$ NOEs were measured from ^1H-detected $^1H-^{13}C$ correlation spectra using the relaxation fitting procedure in Felix (version 2000, Accelrys). All relaxation spectra were recorded with a spectral width of 4494.4 Hz and 1024 complex points in t_2. Digital oversampling by a factor of 40 was employed to reduce baseline distortions associated with the spectrometer's low-pass filters,[51] and all experiments were recorded using the hypercomplex method of phase incrementation to obtain quadrature phase detection in t_1. A spectral width of 3205.2 Hz was used in t_1, leading to extensive folding of the spectrum, and 128 complex points were collected. For the R_1 and R_2 experiment a repetition delay of 4.528 s between transients was used, and the total number of transients recorded per real t_1 point was 64. To measure R_1, nine experiments with relaxation delays T of 0.01, 0.03, 0.06, 0.1, 0.15, 0.2, 0.6, 1.0, and 2.5 s in addition to one duplicate experiment having a relaxation delay of 0.03 s were recorded in an interleaved manner over a 12-day period. Monoexponential evolution of carbon magnetization was obtained by saturation of the protons by applying pulses every 7 ms during the recovery delay in the T1 experiments. The T2 experiment was performed with a Carr−Purcell−Meiboom−Gill (CPMG) spin−echo sequence with 10 transverse relaxation delays of 2, 6, 10, 16, 20, 40, 60, 80, 120, and 250 ms as well as one duplicate relaxation delay of 10 ms recorded in an interleaved manner over a period of 12 days. The CPMG sequence was modified to suppress the effects of cross-correlation between dipolar and chemical shift anisotropy (CSA) relaxation mechanisms.[52] Three independent sets of two spectra, one with and one without ^1H saturation, were recorded to obtain heteronuclear steady-state $\{^1H\}-^{13}C$ NOEs. The ^1H recovery period employed in the NOE measurements was 3.4 s, and the total number of transients recorded per real t_1 point was 128.

Calculation of ModelFree Parameters. All spectra were processed using Felix (version 2000, Accelrys). The spectra were apodized using exponential line broadening as well as a cosine bell function to the first 512 complex data points in each t_2 FID. In t_1 the interferogram was extended to 320 complex points by linear prediction followed by apodization with exponential line broadening and a cosine bell function. Peak height measurements for each spectrum were performed using routines written in the Felix macro programming language. The values of R_1 and R_2 were obtained by employing the relaxation nonlinear least-squares fitting procedures in Felix. NOE values were calculated as the ratios of the peak intensities measured from spectra acquired with and without proton irradiation during the recycle delay.

The extended ModelFree formalism was employed to determine the amplitudes and time scales of the intramolecular motions.[53−56] Motional models for each C−H vector were selected by assessing the residual sum square error for the fit to each model. For model 1, the $\alpha = 0.05$ critical value is approximately $\Gamma = 6.0$, for models 2 and 3, $\Gamma = 3.8$, and for models 4 and 5 in which three parameters are being fitted, Γ is required to be 0. In the cases where it was possible to fit the relaxation data to two or more models, an F test was employed to determine if the more complicated model offered a statistically significant improvement in the fit. All model selections were performed assuming an isotropic overall rotational diffusion tensor. Finally, the internal motion parameters for each spin were optimized assuming an axially symmetric diffusion model using one of the calculated solution structures of the LNA/DNA:RNA duplex.[26] The global correlation time for the duplex was extracted from the final optimization with the selected model for each nuclear spin.

Results and Discussion

Spectral Analysis. The 1D ^1H NMR spectrum of the LNA/DNA:RNA duplex displayed sharp lines from the expected duplex with no signs of alternative structures. The chemical shift values of the protons were assigned using previously reported chemical shifts[24] and 2D NOESY and COSY spectra. The ^{13}C resonances were assigned by correlating the proton chemical shift with the carbon chemical shifts using HSQC and HMQC spectra. The C1′−H1′ region of the HMQC-based spectrum used to obtain the carbon R_1 values is shown in Figure 1a.

The relaxation parameters R_1 and R_2 (Figure 1b) and NOE were determined by analysis of proton-detected natural abundance $^{13}C-^1H$ heteronuclear correlation spectra. The uncertainties of the obtained values were estimated from one duplicate spectrum in the R_1 and R_2 relaxation series, and the NOE uncertainties were determined by analyzing three independent NOE experiments. Relaxation measurements and ModelFree parameters were determined for 79 out of 94 methine spins in the molecule. Of these 79 resolved spins, 45 were from the RNA strand and the remaining 34 from the chimeric LNA/DNA strand. Deoxyribose has three methine carbons, C1′, C3′, and C4′; ribose has four methine carbons, C1′, C2′, C3′, and C4′; and LNA nucleotides have three methine carbons, C1′, C2′, and C3′. LNA does not have a C4′ methine due to the oxymethylene bridge between C2′ and C4′. Consequently, there are a larger number of calculated order parameters for the RNA strand

(51) Delsuc, M. A.; Lallemand, J. Y. *J. Magn. Reson.* **1986**, *69*, 504−507.
(52) Palmer, A. G., III; Skelton, N. J.; Chazin, W. J.; Wright, P. E.; Rance, M. *Mol. Phys.* **1992**, *75*, 699−711.
(53) Palmer, A. G., III; Rance, M.; Wright, P. E. *J. Am. Chem. Soc.* **1991**, *113*, 4371−4380.
(54) Lipari, G.; Szabo, A. *J. Am. Chem. Soc.* **1982**, *104*, 4546−4559.
(55) Lipari, G.; Szabo, A. *J. Am. Chem. Soc.* **1982**, *104*, 4559−4570.
(56) Clore, G. M.; Szabo, A.; Bax, A.; Kay, L. E.; Driscoll, P. C.; Gronenborn, A. M. *J. Am. Chem. Soc.* **1990**, *112*, 4989−4991.

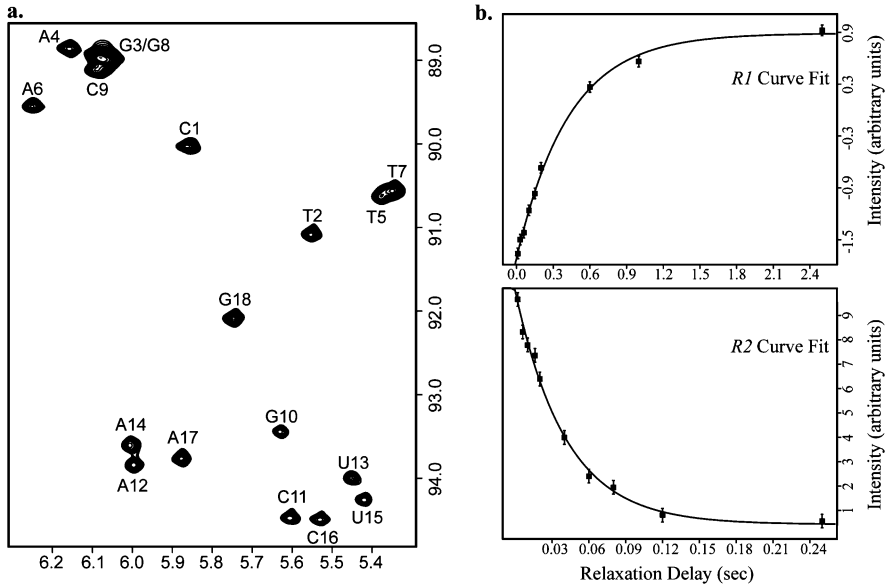

Figure 1. (a) C1′ portion of the $^{13}C-^{1}H$ correlation spectrum used to measure R_1 with a relaxation delay of 10 ms. Due to overlap of the G3C1′ and G8C1′ it was not possible to obtain ModelFree parameters for these spins. (b) ^{13}C relaxation data for A6C1′. (Top) R_1 relaxation decay curve and (bottom) the R_2 relaxation decay curve.

relative to the chimeric LNA/DNA strand. Calculated ^{13}C relaxation data and optimized ModelFree parameters are given in Table 1.

Due to spectral overlap, it was not possible to obtain relaxation data or calculate order parameters for G3C1′ and G8C1′ and all but the four terminal C4′ carbons. The spectral overlap of G3C1′ and G8C1′ is particularly unfortunate, as these two spins are on nucleotides positioned directly 3′ to an LNA residue in the chimeric strand.

The total order parameter, S^2, is a measure of the conformational distribution of a $^{13}C-^{1}H$ vector as it moves relative to the remainder of the molecule. The order parameter ranges from 1 to 0, with a value of 1 indicating an immobile, ordered vector. Lower values of S^2 are indicative of a flexible, more mobile vector whose motion is less correlated with the overall tumbling of the molecule. The order parameter S^2 is therefore associated with motions on the picosecond to nanosecond time scale. The effective correlation time τ_e depends on the rate of motion of the C−H bond vector. A physical interpretation of τ_e is generally difficult and requires reference to a specific motional model. Because the data are insufficient to allow the selection of a particular motional model, we do not make any attempt to interpret the τ_e values calculated from the relaxation data. R_{ex} has been included to account for the effects of chemical exchange and other pseudo-first-order processes such as conformational averaging on a time scale much slower than the overall rotational correlation time (τ_m) that contributes to the decay of transverse magnetization.[58]

A global correlation time for the duplex of 4.7 ns was found for both the isotropic overall diffusion and axially symmetric diffusion models. The axially symmetric diffusion model yielded a $D_{||}/D_{\perp}$ ratio of 1:1.16. Because this ratio is very close to 1, the error introduced by employing an isotropic diffusion model is expected to be very small. A global correlation time of 4.7 ns is at first glance unexpected when considering previous determinations of correlation times in DNA duplexes of approximately the same size. Table 2 summarizes some of the experimental values of correlation times obtained for various DNA duplexes. The discrepancy between the rotational correlation time measured by cross-relaxation and by DDLS may be due to the sensitivity of the NOE cross-peak volume to dynamics, whereas the DDLS method is relatively insensitive to the internal motion in the molecule.[59] The long global correlation time may also arise from self-association between oligomers, possibly transient end-to-end stacking. However, we do not observe any direct evidence for these effects in our spectra, such as "impossible NOEs" between protons on opposite ends of the helix at long NOESY mixing times (data not shown). A theoretical investigation of the effect of dimerization has shown that the presence of dimers in the solutions, even as little as 10% of the total amount of monomers, significantly distorts the results obtained by the original and extended formulation of the ModelFree approach.[60] However, another study argued that even though dimerization leads to an overestimate of the total order parameter, S^2, the relative trends of the order parameters in the protein under investigation should be unaltered.[61] The literature provides conflicting evidence with respect to correlation times for oligomers in solution.

Description of the Total Order Parameter, S^2. Table 3 shows the distribution of the total order parameter in the chimeric LNA/DNA and RNA strands. The average S^2 of the 79 resolved spins for the modified LNA/DNA:RNA duplex is 0.92 ± 0.09, indicating a highly ordered structure. The order of the LNA/DNA:RNA duplex is comparable to or slightly higher than that found in unmodified dsDNA duplexes and RNA hairpin structures (Table 3).

(57) Mandel, A. M.; Akke, M.; Palmer, A. G., III. *J. Mol. Biol.* **1995**, *246*, 144−163.
(58) Bloom, M.; Reeves, L. W.; Wells, E. J. *J. Chem. Phys.* **1965**, *42*, 1615−1624.
(59) Eimer, W.; Williamson, J. R.; Boxer, S. G.; Pecora, R. *Biochemistry* **1990**, *29*, 799−811.
(60) Schurr J. M.; Babcock, H. P.; Fujimoto, B. S. *J. Magn. Res. B* **1994**, *105*, 211−224.
(61) Liu, Q.; Yuan, Y.-C.; Shen, B.; Chen, D. J.; Chen, Y. *Biochemistry* **1999**, *38*, 1415−1425.

Table 1. ^{13}C Relaxation and ModelFree Parameters in the LNA/DNA:RNA Duplex

ATOM	S_{tot}^2	R_1 (s^{-1})	R_2 (s^{-1})	NOE	model	τ_e (ps)	R_{ex} (s^{-1})	SSE
C1:C1′	0.81 ± 0.03	2.30 ± 0.15	19.2 ± 1.35	1.48 ± 0.02	2	132 ± 50	0 ± 0	0.64
T2:C1′	0.95 ± 0.08	2.22 ± 0.18	30.3 ± 2.44	1.20 ± 0.03	3	0 ± 0	9 ± 3	1.89
G3:C1′ [a]								
A4:C1′	0.94 ± 0.05	2.61 ± 0.18	23.4 ± 1.63	1.26 ± 0.07	2	551 ± 566	0 ± 0	2.85
T5:C1′	0.95 ± 0.06	2.23 ± 0.14	30.7 ± 3.36	1.15 ± 0.07	3	0 ± 0	10 ± 4	0.02
A6:C1′	0.94 ± 0.06	2.30 ± 0.18	19.9 ± 1.77	1.09 ± 0.06	1	0 ± 0	0 ± 0	1.85
T7:C1′	0.98 ± 0.05	2.30 ± 0.13	24.7 ± 1.73	1.19 ± 0.07	3	0 ± 0	3 ± 2	0.20
G8:C1′ [a]								
C9:C1′	0.91 ± 0.05	2.13 ± 0.12	22.8 ± 1.30	1.26 ± 0.11	3	0 ± 0	3 ± 2	0.87
G10:C1′	0.82 ± 0.08	1.92 ± 0.19	38.7 ± 3.86	1.03 ± 0.11	3	0 ± 0	21 ± 4	1.48
C11:C1′	1.00 ± 0.11	2.43 ± 0.26	25.8 ± 2.27	1.13 ± 0.06	3	0 ± 0	3 ± 3	0.24
A12:C1′	0.90 ± 0.07	2.11 ± 0.17	32.2 ± 2.77	1.17 ± 0.11	3	0 ± 0	12 ± 3	0.01
U13:C1′	0.93 ± 0.09	2.17 ± 0.20	31.7 ± 2.93	1.07 ± 0.07	3	0 ± 0	11 ± 3	1.57
A14:C1′	0.98 ± 0.09	2.29 ± 0.20	29.5 ± 2.62	1.16 ± 0.07	3	0 ± 0	8 ± 3	0.00
U15:C1′	0.99 ± 0.09	2.31 ± 0.21	31.8 ± 2.87	1.11 ± 0.10	3	0 ± 0	10 ± 3	0.26
C16:C1′	0.96 ± 0.08	2.24 ± 0.18	30.3 ± 2.40	1.19 ± 0.11	3	0 ± 0	9 ± 3	0.07
A17:C1′	0.95 ± 0.07	2.23 ± 0.16	33.1 ± 2.41	1.17 ± 0.11	3	0 ± 0	12 ± 3	0.01
G18:C1′	0.87 ± 0.04	2.31 ± 0.12	16.3 ± 1.81	1.28 ± 0.03	2	59 ± 26	0 ± 0	3.78
T2:C2′	0.93 ± 0.06	2.18 ± 0.18	20.3 ± 1.93	1.31 ± 0.10	1	0 ± 0	0 ± 0	2.48
T5:C2′	0.97 ± 0.09	2.28 ± 0.21	28.9 ± 3.00	1.11 ± 0.11	3	0 ± 0	7 ± 4	0.23
T7:C2′	0.97 ± 0.06	2.09 ± 0.17	23.2 ± 2.11	1.13 ± 0.16	3	0 ± 0	4 ± 3	0.04
G10:C2′	0.99 ± 0.07	2.24 ± 0.22	22.9 ± 2.72	1.11 ± 0.04	1	0 ± 0	0 ± 0	1.83
C11:C2′	0.97 ± 0.11	2.27 ± 0.25	33.6 ± 5.54	1.07 ± 0.08	3	0 ± 0	12 ± 6	1.22
A12:C2′	0.88 ± 0.09	2.06 ± 0.20	28.0 ± 3.28	1.10 ± 0.07	3	0 ± 0	9 ± 4	0.74
U13:C2′	1.00 ± 0.07	2.43 ± 0.16	24.5 ± 4.46	1.14 ± 0.03	3	0 ± 0	2 ± 5	0.53
A14:C2′	1.00 ± 0.08	2.24 ± 0.21	24.3 ± 3.17	1.02 ± 0.07	1	0 ± 0	0 ± 0	5.32
U15:C2′	1.00 ± 0.09	2.39 ± 0.22	33.8 ± 5.72	1.16 ± 0.09	3	0 ± 0	11 ± 6	0.00
C16:C2′	0.96 ± 0.06	2.25 ± 0.14	27.1 ± 2.42	1.16 ± 0.04	3	0 ± 0	6 ± 3	0.00
A17:C2′	1.00 ± 0.09	2.39 ± 0.21	21.4 ± 5.00	1.07 ± 0.05	3	0 ± 0	0 ± 5	3.21
G18:C2′	0.66 ± 0.05	2.81 ± 0.14	15.4 ± 1.00	1.53 ± 0.15	2	305 ± 73	0 ± 0	1.18
C1:C3′	0.88 ± 0.06	2.40 ± 0.21	20.2 ± 2.43	1.39 ± 0.10	2	174 ± 167	0 ± 0	0.06
T2:C3′	1.00 ± 0.08	2.29 ± 0.23	26.3 ± 3.22	0.96 ± 0.12	1	0 ± 0	0 ± 0	4.28
G3:C3′	0.72 ± 0.08	2.86 ± 0.29	15.1 ± 2.02	1.27 ± 0.04	2	1000 ± 297	0 ± 0	2.65
A4:C3′	0.90 ± 0.07	2.37 ± 0.23	17.0 ± 2.32	1.19 ± 0.07	1	0 ± 0	0 ± 0	2.97
T5:C3′	1.00 ± 0.07	2.52 ± 0.21	21.6 ± 2.24	1.17 ± 0.10	1	0 ± 0	0 ± 0	0.52
A6:C3′	0.86 ± 0.09	2.02 ± 0.21	27.4 ± 4.10	1.05 ± 0.11	3	0 ± 0	8 ± 5	1.03
T7:C3′	1.00 ± 0.06	2.34 ± 0.16	23.6 ± 2.27	1.08 ± 0.07	1	0 ± 0	0 ± 0	1.76
G8:C3′	0.79 ± 0.05	2.45 ± 0.19	18.2 ± 1.75	1.54 ± 0.10	2	172 ± 84	0 ± 0	0.02
C9:C3′	0.63 ± 0.04	1.71 ± 0.10	15.1 ± 1.23	1.50 ± 0.10	2	36 ± 11	0 ± 0	1.04
G10:C3′	0.99 ± 0.11	2.31 ± 0.26	41.2 ± 5.99	1.10 ± 0.16	3	0 ± 0	19 ± 6	0.15
C11:C3′	1.00 ± 0.10	2.34 ± 0.24	31.9 ± 4.45	1.17 ± 0.14	3	0 ± 0	10 ± 5	0.00
A12:C3′	1.00 ± 0.11	2.40 ± 0.20	28.4 ± 4.63	1.11 ± 0.08	3	0 ± 0	6 ± 5	0.38
U13:C3′	1.00 ± 0.12	2.44 ± 0.27	25.0 ± 5.43	1.16 ± 0.01	3	0 ± 0	2 ± 6	0.00
A14:C3′	1.00 ± 0.08	2.52 ± 0.23	20.1 ± 2.87	1.13 ± 0.15	1	0 ± 0	0 ± 0	1.07
U15:C3′	0.91 ± 0.09	2.55 ± 0.30	16.3 ± 2.74	1.11 ± 0.19	1	0 ± 0	0 ± 0	3.96
C16:C3′	1.00 ± 0.08	2.31 ± 0.24	24.3 ± 3.14	1.07 ± 0.05	1	0 ± 0	0 ± 0	3.53
A17:C3′	0.80 ± 0.07	2.00 ± 0.22	19.2 ± 2.99	1.32 ± 0.05	2	43 ± 23	0 ± 0	0.28
G18:C3′	0.77 ± 0.05	2.65 ± 0.16	16.5 ± 1.42	1.47 ± 0.07	2	336 ± 103	0 ± 0	1.44
C1:C4′	0.82 ± 0.05	2.16 ± 0.18	17.5 ± 1.68	1.31 ± 0.04	2	47 ± 20	0 ± 0	0.31
C9:C4′	0.97 ± 0.07	2.23 ± 0.18	23.1 ± 3.51	1.29 ± 0.14	1	0 ± 0	0 ± 0	1.13
G10:C4′	1.00 ± 0.08	2.33 ± 0.24	22.8 ± 2.57	1.28 ± 0.08	1	0 ± 0	0 ± 0	2.48
G18:C4′	0.99 ± 0.09	2.45 ± 0.23	18.5 ± 3.66	1.20 ± 0.03	1	0 ± 0	0 ± 0	2.57
C1:C6	1.00 ± 0.11	3.32 ± 0.36	63.4 ± 7.61	1.24 ± 0.18	3	0 ± 0	31 ± 8	0.45
C1:C5	0.79 ± 0.06	2.52 ± 0.19	27.5 ± 2.03	1.09 ± 0.04	3	0 ± 0	3 ± 3	0.52
T2:C6	1.00 ± 0.12	3.27 ± 0.38	47.5 ± 5.60	1.18 ± 0.16	3	0 ± 0	16 ± 7	0.16
G3:C8	0.91 ± 0.14	2.21 ± 0.41	32.9 ± 7.94	0.94 ± 0.14	1	0 ± 0	0 ± 0	3.77
A4:C8	1.00 ±0.18	3.33 ± 0.54	40.4 ± 9.86	1.25 ± 0.13	1	0 ± 0	0 ± 0	1.31
A4:C2	1.00 ± 0.15	3.21 ± 0.49	70.4 ± 11.8	1.07 ± 0.08	3	0 ± 0	39 ± 13	0.37
T5:C6	0.99 ± 0.07	3.38 ± 0.32	28.4 ± 3.24	1.12 ± 0.10	1	0 ± 0	0 ± 0	0.94
A6:C8	1.00 ± 0.11	2.97 ± 0.35	30.8 ± 5.20	1.07 ± 0.07	1	0 ± 0	0 ± 0	1.20
A6:C2	0.85 ± 0.07	2.73 ± 0.22	25.6 ± 2.78	1.11 ± 0.08	3	0 ± 0	0 ± 3	0.11
T7:C6	0.96 ± 0.08	2.71 ± 0.29	40.0 ± 4.97	1.11 ± 0.08	1	0 ± 0	0 ± 0	5.77
G8:C8	1.00 ± 0.17	2.97 ± 0.46	38.6 ± 7.13	1.16 ± 0.06	3	0 ± 0	10 ± 8	0.10
C9:C6	0.92 ± 0.11	2.95 ± 0.36	48.4 ± 7.23	1.03 ± 0.13	3	0 ± 0	20 ± 8	0.49
C9:C5	0.90 ± 0.07	2.89 ± 0.23	33.6 ± 2.76	1.28 ± 0.11	3	0 ± 0	6 ± 4	2.18
G10:C8	0.95 ± 0.18	2.56 ± 0.48	28.1 ± 8.69	1.18 ± 0.17	3	0 ± 0	4 ± 10	0.05
C11:C6	0.94 ± 0.10	3.01 ± 0.31	59.2 ± 6.74	1.27 ± 0.21	3	0 ± 0	30 ± 7	0.54
C11:C5	0.88 ± 0.08	2.82 ± 0.25	32.2 ± 3.23	1.09 ± 0.10	3	0 ± 0	5 ± 4	0.08
A12:C8	0.93 ± 0.14	2.50 ± 0.37	44.0 ± 6.29	1.14 ± 0.17	3	0 ± 0	20 ± 7	0.00
A12:C2	0.93 ± 0.11	2.98 ± 0.34	58.7 ± 5.95	1.03 ± 0.06	3	0 ± 0	30 ± 7	1.99
U13:C6	0.69 ± 0.13	2.34 ± 0.58	29.9 ± 7.65	1.44 ± 0.13	2	68 ± 53	0 ± 0	1.55
U13:C5	0.70 ± 0.07	2.25 ± 0.22	31.7 ± 3.06	1.09 ± 0.12	3	0 ± 0	10 ± 4	0.05
A14:C8	0.76 ± 0.12	2.10 ± 0.36	17.9 ± 6.02	1.11 ± 0.11	1	0 ± 0	0 ± 0	0.17
A14:C2	0.83 ± 0.07	2.66 ± 0.23	42.5 ± 5.45	1.05 ± 0.06	3	0 ± 0	17 ± 6	1.30
U15:C6	0.82 ± 0.10	2.84 ± 0.46	22.9 ± 4.62	1.03 ± 0.08	1	0 ± 0	0 ± 0	1.79
U15:C5	0.85 ± 0.07	2.59 ± 0.26	30.0 ± 4.14	1.06 ± 0.05	1	0 ± 0	0 ± 0	2.63
C16:C6	0.88 ± 0.10	2.81 ± 0.33	50.9 ± 7.51	1.19 ± 0.19	3	0 ± 0	24 ± 8	0.15
C16:C5	0.90 ± 0.08	2.87 ± 0.27	33.5 ± 3.54	1.12 ± 0.08	3	0 ± 0	6 ± 4	0.00
A17:C8	0.91 ± 0.15	2.44 ± 0.39	37.8 ± 7.05	1.12 ± 0.16	3	0 ± 0	15 ± 8	0.02
A17:C2	0.88 ± 0.08	2.82 ± 0.26	45.4 ± 5.24	1.01 ± 0.06	3	0 ± 0	18 ± 6	3.27
G18:C8	1.00 ± 0.12	2.52 ± 0.38	30.7 ± 5.65	1.10 ± 0.03	1	0 ± 0	0 ± 0	2.37

[a] Due to spectral overlap, no relaxation data could be determined for G3:C1′ and G8:C1′. Model selection is described by Mandel et al.[57]

Table 2. Experimental Values of the Correlation Times in DNA Duplexes

sequence	τm (ns)	method	reference
d(TCGCG)2	0.9	NMR (ModelFree)	47
d(CGCGCG)2	1.4	NMR (ModelFree)	47
d(CGCTAGCG)2	3.4	NMR (ModelFree)	43
d(GCGTACGC)2	3.7	NMR (ModelFree)	41
d(CCACGCGTGG)2	5.3	NMR (ModelFree)	42
d(CGCAAATTTGCG)2	3.7	NMR (ModelFree)	62
d(CGCGCGCG)2	3.2	DDLS[a]	59
d(CGCGCGCG)2	1.2	NMR (CR)[b]	59
d(CGCGCGCGCGCG)2	6.4	DDLS[a]	59
d(CGCGCGCGCGCG)2	3	NMR (CR)[b]	59

[a] Depolarized dynamic light scattering. [b] Measured by cross-relaxation rates of the cytosine H5−H6.

Table 3. Average Values of S^2 Measured in the LNA/DNA:RNA Duplex in Addition to Previously Determined Values in dsDNA Duplexes[a]

	aromatic	sugar
all	0.90 ± 0.09	0.92 ± 0.09
LNA	0.98 ± 0.02	0.96 ± 0.04
DNA	0.94 ± 0.08	0.85 ± 0.10
RNA	0.87 ± 0.09	0.94 ± 0.09
8-mer DNA[41]	0.83 ± 0.06	0.75 ± 0.13
8-mer DNA[43]	0.79 ± 0.06	0.76 ± 0.12
10-mer DNA[42]	0.93 ± 0.07	0.86 ± 0.11
ΔTAR RNA[44]	0.73 ± 0.11	
UUCG RNA[45]	0.77 ± 0.02	
IRE RNA (20 °C)[46]	0.76 ± 0.02	
IRE RNA (30 °C)[46]	0.77 ± 0.07	

[a] Values are given plus/minus one standard deviation.

As shown in Table 3, the aromatic spins in the RNA strand have larger amplitudes of motion than those in the LNA/DNA strand. On the other hand, the sugar rings in the RNA and LNA residues are more ordered than those of the DNA nucleotides in the LNA/DNA chimera. The global average order parameter of the DNA sugars agrees with those previously found in an unmodified 10-mer DNA duplex.[42] The high order in the LNA/DNA:RNA was predicted by unrestrained molecular dynamics trajectories of both RNA duplexes and hybrid DNA:RNA duplexes. These computational studies showed that A-RNA tends to be much more rigid than B-DNA.[63,64] However, experimental data available for RNA hairpins[44−46] reveal a somewhat lower order for the RNA aromatic spins compared to the LNA/DNA:RNA duplex. Interestingly, the order parameters for aromatic spins in unmodified DNA duplexes have been found to be both higher and lower than those for RNA. Unfortunately, the experimentally determined order parameters reported for the RNA hairpin structures do not include data for the sugar methines.

A graphical representation of some of the order parameters measured in each nucleotide is shown in Figure 2.

Order Parameters for the Aromatic Spins. The bases in the LNA/DNA chimeric strand are uniformly and highly ordered (Figure 2a). In contrast, there is an abrupt decrease in order for the bases in the RNA strand at U13:A6. The order of the bases 3′ to the U13:A6 basepair increases monotonically for the remaining nucleotides in the RNA strand (Figure 2b).

The U13:A6 base pair is flanked by two LNA/DNA:RNA base pairs. Both the A12C8 and A12C2 methines are highly ordered with an $S^2 = 0.93$. The U13C6 ($S^2 = 0.69$) and U13C5 ($S^2 = 0.70$) methines are significantly less ordered.

Direct comparison of the order of the LNA/DNA:RNA to normal RNA duplex is difficult because there are few reports of experimentally determined order parameters for RNA in the literature.[44−46] The UUCG hairpin RNA has been investigated by Akke et al. using ^{15}N relaxation measurements of imino N−H vectors and interpreted as order parameters.[45] Interestingly, the bases in the stem region have very uniform order in the range of $S^2 = 0.8$. In comparison with the order in the aromatic bases of the RNA strand in the LNA/DNA:RNA system, the profound decrease in order for U13 relative to the LNA/DNA chimera and the majority of the bases in the RNA strand looks more like a return to normal dynamics. The uridine imino vector has the same angular relationship to the glycosidic bond as does the C5 methine; however, the imino points into the center of the helix while the C5 methine points out into the solvent. Akke et al. provide the caveat for their analysis that the CSA for the uridine imino is not known, and therefore the order parameter must be treated with caution. However, their measurements for the guanine imino order, for which a good estimate of the CSA is known, are in good agreement with the uridine order. If the ^{13}C and ^{15}N relaxation are adequately sampling the spectral density function for these molecules, it appears that hybridization of the LNA/DNA chimera to the RNA strand induces a significant increase in the order of the entire molecule.

The King group has reported ^{13}C order parameters for the C8/C6 methine spins in the ΔTAR RNA molecule.[44] For bases involved in duplex, Watson−Crick base pairing, the average order for purines is 0.79, for pyrimidines 0.68, and for the duplex Watson−Crick base pairs as a whole $S^2 = 0.73$. The range of order parameters for the aromatic spins in the ΔTAR duplex regions is $S^2 = 0.56-1.0$. In particular, two of the three uridine residues in duplex regions have $S^2 = 0.67$, very similar to the LNA/DNA:RNA U13C6 spin $S^2 = 0.69$. These results are in good agreement with the ^{15}N-derived order parameters obtained by Akke et al.[45] Comparing the available order parameters for the bases from previous DNA and RNA studies with those found for the LNA/DNA:RNA duplex, we conclude that the LNA residues dramatically increase the order of the duplex. The order parameter provides an estimate of the configurational entropy contribution to the duplex formation.[65,66] The preferred conformation for an RNA:DNA hybrid lies toward the A-form family. This requires a reorganization of the DNA strand from its preferred B-form conformation to an energetically less favorable A-form-like conformation. This is reflected in the T_m of the various duplexes. The inclusion of LNA into the DNA chimera has a profound effect on the thermal stability of the resulting LNA/DNA:RNA hybrid. The T_m of the LNA/DNA:RNA hybrid is 52 °C, whereas the melting temperature of the corresponding DNA:RNA and DNA:DNA molecules is approximately 28 °C. We suggest that part of the substantial increase in T_m for the LNA/DNA:RNA hybrid is due to the preorganization of the

(62) Gaudin, F.; Chanteloup, L.; Thuong, N. T.; Lancelot, G. *Magn. Res. Chem.* **1997**, *35*, 561−565.
(63) Cheatham, T. E.; Kollman, P. A. *J. Am. Chem. Soc.* **1997**, *119*, 4805−4825.
(64) Auffinger, P.; Westhof, E. *J. Mol. Biol.* **2000**, *300*, 1113−1131.
(65) Akke, M.; Brüschweiler, R.; Palmer, A. G., III. *J. Am. Chem. Soc.* **1993**, *115*, 9832−9833.
(66) Yang, D.; Kay, L. E. *J. Mol. Biol.* **1996**, *263*, 369−382.

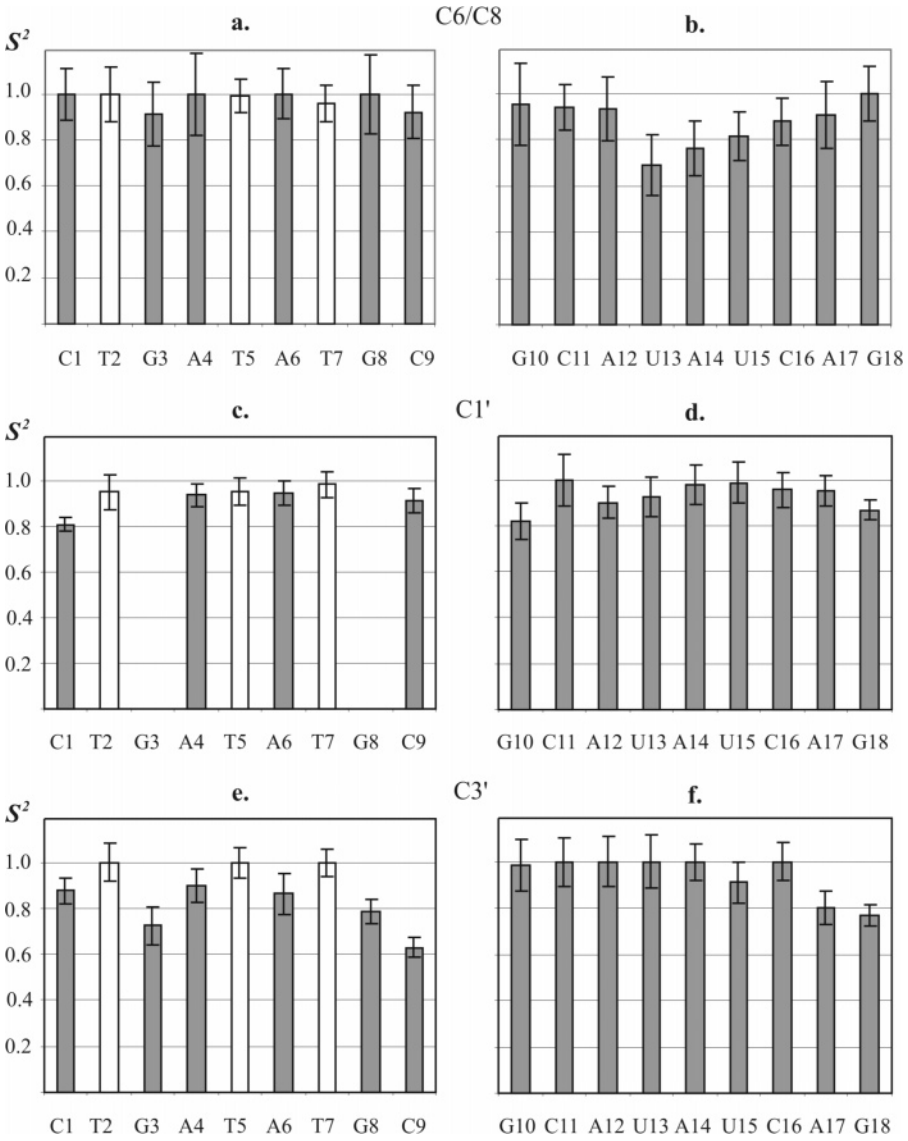

Figure 2. Calculated order parameters for the C6/C8, C1′, and C3′ carbons in the LNA/DNA strand (left) and the RNA strand (right). White bars indicate the LNA modified nucleotides.

DNA strand to the A-form conformation. We have previously demonstrated conformational coupling between residues in DNA.[67]

Order Parameters for the Sugar Spins. Unfortunately, there are no published order parameters available for the ribose spins in duplex RNA. Therefore, we can make no comparison between normal dsRNA and the RNA strand of the LNA/DNA:RNA duplex. In the previous structural analysis of the LNA/DNA:RNA and the unmodified DNA:RNA duplex, it was found that the *N*-type conformation adopted by the riboses in the RNA component of the unmodified DNA:RNA duplex greatly affects the overall conformation of the duplex.[24,26] Conformational coupling through the aromatic bases from one strand to the other appears to transmit the *N*-type sugar conformations of the RNA strand to the more plastic DNA strand. The observed *N*-type sugar conformation in the DNA strand arises since the DNA nucleotides can adopt either an *N*- or *S*-type sugar conformation with little energetic penalty. As a result, the unmodified DNA:RNA duplex was found to have an overall RNA-like appearance.[26] In the LNA modified duplex, where conformationally restricted LNA nucleotides have been interspersed between the more plastic deoxyribonucleotides, it has been found from DQF-COSY studies that a conformational coupling exists between LNA and adjacent unmodified sugars,[24] leading to an even more pronounced A-form overall structure. The current study emphasizes the dynamic aspects of this conformational coupling.

The order parameters for the sugar C−H vectors in the LNA nucleotides are all close to 1 as expected for the rigid, locked sugar ring and additionally indicate that the LNA residues do not undergo any apparent rigid body motion of the sugar relative to the rest of the molecule. The RNA nucleotides show the same trend with highly ordered ribose rings as judged by the available data on the C1′, C2′, and C3′ spins. An interesting observation that confirm others previously made in unmodified DNA duplexes[41−43] is that the terminal sugars are quite ordered (C1′ and C4′), and it is the 3′ end C3′ that is highly mobile.

The relative population of *N*- and *S*-type sugar conformations is a fairly easily obtainable measure of the dynamics in the deoxyribose rings. In an earlier analysis, employing PSEUROT

(67) Isaacs, R. J.; Spielmann, H. P. *J. Mol. Biol.* **2001**, *307*, 525−540.

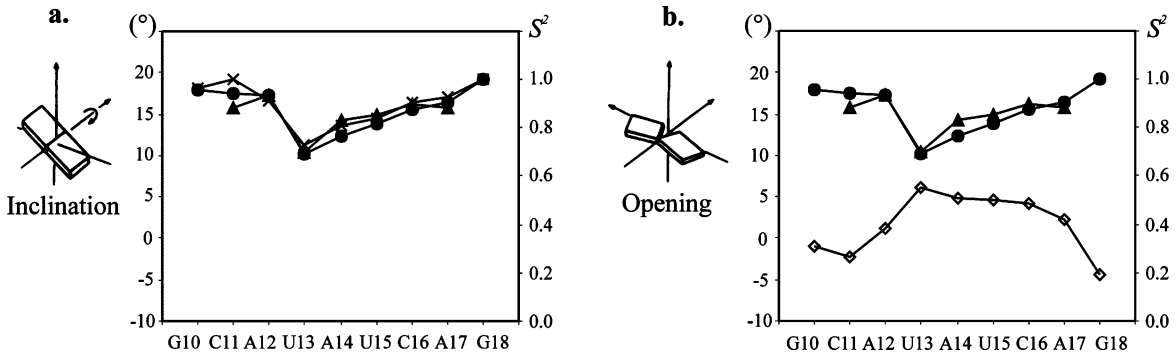

Figure 3. Total order parameter, S^2, in the RNA strand for C6/C8 (●) and C2/C5 (▲), and the structural parameters (a) inclination (×) and (b) opening (◇). Note the different scales for the order and helical parameters.

and coupling constants derived from a DQF-COSY spectrum, it was concluded that the *N*-type populations of all but the terminal nucleotides in the LNA strand were above 90%.[24] In the context of dsDNA, it has previously been concluded that the LNA nucleotide perturbs the *N*/*S* sugar conformational equilibrium of neighboring unmodified DNA nucleotides in favor of *N*-type conformations.[23] This effect is most pronounced for DNA nucleotides sandwiched between LNA nucleotides, yielding almost pure *N*-type sugars. A smaller effect on conformational preference is observed for 3′-neighboring DNA nucleotides, and the least effect is seen for 5′ neighboring DNA nucleotides.

A free deoxyribose in solution is conformationally quite mobile. Polymerization of deoxyribonucleotides and subsequent formation of a double helical structure reduces this conformational freedom by enforcing energetic coupling of adjacent inter- and intrastrand sugars in dinucleotide units. The interstrand coupling is mediated by base-pairing and base-stacking interactions. These couplings will be transmitted from the bases through the glycosidic linkages to the sugars. The intrastrand coupling is mediated through the conformations of the intervening torsion angles between two neighboring sugars in a dinucleotide unit. The inclusion of conformationally restricted LNA residues in a DNA strand will block some of this concerted motion between dinucleotide units and will therefore be expected to have a large impact on adjacent deoxyribonucleotides. As seen in Figure 2e, the order parameters of the C3′ atoms in the LNA/DNA strand display a more dynamic picture. This mirrors the situation in unmodified DNA, in which the C3′ atoms constitute the conformationally most labile position. However, it is important to note that the order for all of the spins in this strand is still quite high, further demonstrating the effect of conformational restriction of the DNA sugar residues by the presence of the interspersed LNA. The order parameters for G3:C3′ and G8:C3′ atoms are somewhat lower than the rest of the C3′s, indicating a slightly higher mobility of these atoms compared to the other C3′ atoms in the LNA strand. These nucleotides are both 3′-neighbors to LNA modifications. Interpretation of deoxyribose sugar ^3J-(^{1}H−^{1}H) coupling constants in other LNA/DNA chimeras suggests that there is an apparent increase in conformational freedom for deoxynucleotides on the 3′ side of LNA.[23,24] The lower order parameters observed for the G3:C3′ and G8:C3′ spins confirm this observation and indicate that relatively greater conformational freedom is retained by the deoxyribose 3′ flanking nucleotides of the LNA/DNA:RNA duplex.

This interpretation of the order parameters for the sugar atoms of the LNA/DNA:RNA duplex suggests the conformational coupling of adjacent nucleotides. In this model, the conformational interconversion of one sugar affects the possible conformations of the adjacent sugars through the torsions of the intervening bonds, through the existence of water-mediated hydrogen bridges, or possibly through a combination of both effects.

Correlations between Structural Parameters and Local Dynamics. A number of possible explanations of the increased A-like geometry in LNA-containing duplexes have been proposed, including a restriction of the sugar−phosphate backbone, steric restrictions imposed by the inclusion of the 2′-oxymethylene bridge of the LNA sugars, maximization of the nucleobase stacking leading to the locked A-type LNA imposing A-like geometry on the neighboring DNA nucleobase, the existence of a water-mediated hydrogen bond between the O2′ on the LNA nucleotide and the O4′ on the 3′-flanking DNA sugar, and an altered charge distribution in the minor groove.[26] A shift to an A-form structure is a common feature of the LNA chimeras studied to date. The structural strain introduced by the altered sugar conformational equilibrium in these molecules is relieved by the partial unwinding of the helix and widening of the minor groove. The helical parameters calculated for these systems also progressively shift toward values characteristic for A-form duplexes as more LNA nucleotides are incorporated into the duplex.[21,22,25,26] However, it should be noted that some of the variations in the helical parameters within a given duplex are sequence-dependent and not directly related to the LNA sugar.

The dynamic parameters obtained from ^{13}C relaxation data evaluated by the ModelFree approach have previously been shown to correlate with a number of helical parameters obtained from analysis of NOE-based duplex DNA solution structures.[42,67] A similar situation exists for the LNA/DNA:RNA duplex where a number of correlations between structural and dynamic features were found. Analysis of the correlations between the obtained order parameters for each C−H vector in the duplex and the structural parameters, calculated by CURVES, was carried out by calculating the Pearson correlation coefficients and evaluating the plausibility of a correlation employing a T test ($\alpha = 0.05$).[68]

The C8/C6 spins on the RNA strand show an almost perfect positive correlation with the base-pair−axis inclination ($r =$

(68) Zar, J. H. *Biostatistical Analysis*, 4th ed.; Prentice-Hall: Upper Saddle River, NJ, 1999.

0.97). In addition, a negative correlation with base−base opening ($r = -0.89$) was observed (Figure 3).

The positive correlation between the base-pair−axis inclination and the order parameter of the aromatic spins means that a lower degree of order of the C6/C8 spins correlates with a lower value of inclination. Typical values of inclination are −5.9° and 19.1° in B- and A-form helices, respectively. As seen in Figure 3, the high values of the order parameter are consistent with values of the inclination close to canonical A-form duplexes, whereas base-pair−axis inclinations intermediate of those seen in A- and B-form helices occur concomitantly with a lower order parameter. The typical values of opening in both A- and B-form duplexes lie around −4.5°, and it is shown in Figure 3b that as the value of opening diverges from the typical value in canonical duplexes, the order parameter decreases, indicating a larger degree of disorder in the aromatic C−H vectors. In both cases, it can be concluded that the dynamics of the aromatic bases are increasingly affected as the structure subtly diverges from canonical helical geometries. Alternatively, the altered dynamics leads to the structural differences observed for the modified duplex. It is not possible to distinguish these two cases with the available data. These structural and dynamical correlations can be further interpreted to be a consequence of enforcement of A-form geometry by conformational coupling of the LNA residues both within the strand and across the helix. The preferred conformation of the RNA strand and LNA residues is a canonical A-form duplex, and the correlation of the aromatic order parameter with inclination is describing the extent of A-form enforcement. The negative correlation of the order parameters with opening of the bases could be an indication of the local helix attempting to remain in B-form but is being forced into an A-form as the LNA nucleotides impose their A-form preference onto the unmodified DNA nucleotides. Effectively, a smaller set of conformations is available to the deoxyriboses in the LNA/DNA chimera leading to a higher order with a smaller opening.

The seven aromatic C5/C2 spins in the RNA strand and the four aromatic C5/C2 spins in the LNA strand were grouped together in the analysis based on their similar angle relationship to the axis defined by the glycosidic bond.[67] Due to the low number of observations in the LNA strand, no statistically significant correlations were found. In the RNA strand, the order parameters of C5/C2 were correlated with base-pair−axis inclination ($r = 0.82$) and base−base stagger ($r = -0.76$).

The C5/C2 and the C6/C8 within the same nucleotide are very well-correlated ($r = 0.82$) when the 5′-terminal C1 nucleotide C6 and C5 spins are excluded. This is expected due to the fixed covalent geometry between these aromatic spins. The apparent discrepancy between the C6 ($S^2 = 1.00$) and C5 ($S^2 = 0.79$) for the 5′-terminal nucleotide can be explained by a motion in which the C5−H5 vector undergoes a displacement, which changes its angular relationship, while the C6−H6 vector is not displaced. If the dot product of the time-dependent orientation of the C6−H6 vector is zero, no additional relaxation takes place, and therefore it will have a higher order than the C5−H5 vector.

The most significant correlation observed for the sugar C−H vectors is the tight correlation ($r = -0.93$) between C1′ order in the LNA strand and the average pseudorotation angle measured on the solution structures. A similar correlation with

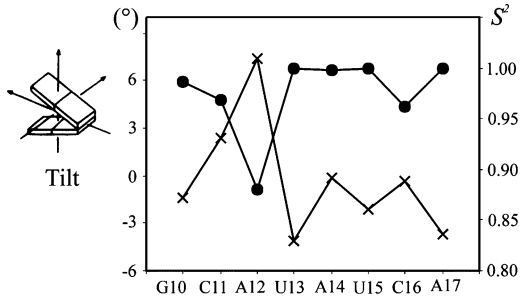

Figure 4. Global interbase pair tilt (×) and the order parameter of C2′ in the RNA strand (●).

the order parameters in the RNA strand was not observed. This once more reflects the conformational forcing of the structure toward a canonical A-form duplex due to the conformational coupling in the LNA/DNA strand. We speculate that the loss of entropy is thus much smaller upon duplex formation than with a native, unmodified DNA strand, and this is further mirrored in the high T_m of the LNA/DNA:RNA duplex.

The global interbase pair parameter tilt was seen to correlate negatively ($r = -0.92$) with the C2′ in the 5′ base in the RNA strand of the base pair step (Figure 4). When the plots in Figure 4 are examined more closely, the correlation is seen to stem from the sharp increase in tilt in the A12pU13:A6pT^{L}7 base pair step. The remaining base pair steps are seen to have values of tilt close to the typical value of 0° seen in regular duplexes and at the same time uniformly high order parameters. The A12pU13 base pair step constitutes the beginning of the central AUAU stretch, which was shown to display a lower degree of order with respect to the aromatic bases. U13C6 displays the lowest order parameter of all the aromatic spins.

Thus, the structural perturbations in the AUAU stretch of the RNA strand are transferred to the sugar spins, and the largest effect is seen at the beginning of the central sequence. As the structure compensates for the altered structural parameters associated with the AUAU:AT^{L}AT^L tract, the order parameters gradually increase throughout the remainder of the sequence as exemplified by the aromatic spins in the RNA strand. This is consistent with the notion that the A6:U13 base pair is the most normal A-form base pair because the A6 deoxyribose conformation is forced by conformational coupling to the adjacent LNA to be almost totally in the *N*-type conformation. As a result, the RNA strand can act like RNA at this base pair and show an order parameter of U13C6 of $S^2 = 0.65$, which is wholly consistent with the dsRNA aromatic order parameters found by previous studies of RNA structures.[44−46]

Conclusions

All the bases in the LNA/DNA strand are highly ordered, whereas the bases in the beginning of the AUAU stretch in the RNA strand display a drop in the aromatic order parameters to levels typical for normal duplex RNA. The comparative decrease in order is most pronounced for the A6:U13 base pair. We suggest that the reason for this decrease in dynamics relative to the rest of the molecule is most likely related to the A6:U13 base pair having the greatest similarity to a normal RNA base pair. This is possibly due to the deoxyribose of A6 being forced by its two flanking LNA nucleotides to adopt an almost pure *N*-type conformation and thereby mimic an RNA nucleotide. The decrease in the order parameter at this base pair thus

signifies a return to normal dynamics typical for dsRNA structures. A consequence of this observation is that higher thermal stability of chimeric LNA/DNA:RNA hybrids may result from substituting LNA for deoxyribose every third base, rather than every second base as at this step.

The severely restricted internal mobility of the interspersed LNA nucleotides prevents the facile conformational interconversion of adjacent deoxyribose residues because they are mechanically coupled. Consequently, the high frequency dynamics of both strands are significantly damped. The interconversion of internucleotide distances and torsion angles involves the concerted displacement of atoms relative to each other. Because the LNA is effectively rigid, it cannot absorb these deformations and therefore presents a higher barrier to vibrations that involve coupled dinucleotide units.

We have shown that the LNA/DNA:RNA hybrid exhibits a range of nucleotide mobilities similar to that observed in globular proteins, and that mobilities of the spins in the bases and sugars correlate with important structural and functional features of the RNA. Hybrid formation between the LNA/DNA chimera and RNA results in a significant rigidification of the residues in the duplex. Our results agree with previous structural studies using NMR and provide an added dynamic aspect to the view of duplex stability due to conformational coupling of the rigid LNA sugar with the adjacent deoxyriboses. Issues not clearly addressed by the current study are the exact mechanism for the conformational change, the connection between the rates, and the thermodynamics of recognition and binding affinity.

Acknowledgment. This work was supported by NSF Grant MCB-9808633, awarded to H.P.S. The Nucleic Acid Center is funded by The Danish National Research Foundation for studies on nucleic acid chemical biology. Britta M. Dahl is thanked for the synthesis of the LNA and RNA strands.

Supporting Information Available: Complete ref 17. This material is available free of charge via the Internet at http://pubs.acs.org.

JA051026Z